Effect of Surface Stress Induced Curvature on Dynamic Response of Triangular Shaped Microcantilevers

Guiming Zhang[1], Libo Zhao[1,#], Zhuangde Jiang[1], Enze Huang[1], Yulong Zhao[1], Xiaopo Wang[2] and Zhigang Liu[2]

1 State Key Laboratory for Manufacturing Systems Engineering, Xi'an Jiaotong University, Xi'an, 710049, China
2 State Key Laboratory of Multiphase Flow in Power Engineering, Xi'an Jiaotong University, Xi'an, 710049, China
Corresponding Author / E-mail: libozhao@mail.xjtu.edu.cn , TEL: +86-29-8266-8616, FAX: +86-29-8339-5139

KEYWORDS : Surface stress, Curvature, Resonant frequency, Triangular shaped microcantilever, Formula

Microcantilevers have played a vital role in chemical and biological detection, especially the triangular shaped microcantilevers for their much higher sensitivity and better anti-twisting capability. Microcantilevers bend in response to differential surface stress. Surface stress can be overwhelming and often play an important role for microcantilevers due to the increasing surface to volume ratio as microcantilevers scale down. This paper gives a detailed theoretical study on surface stress induced curvature and the effect of curvature upon the dynamic response of triangular shaped microcantilevers. The remarkably precise analytical formula for calculating the fundamental resonant frequency of curved triangular shaped microcantilever is validated with FEM (Finite Element Method) results. A very good agreement is obtained between the theoretical results and the FEM results. This formula raises a new perspective that surface stress can be calculated from the fundamental resonant frequency of curved microcantilever using readily measurable microcantilever properties, such as its geometry, elastic modulus and density.

Manuscript received: January XX, 2011 / Accepted: January XX, 2011

NOMENCLATURE

σ = surface stress
E^* = biaxial modulus
E = elastic modulus
v = Poisson's ratio
d = thickness of microcantilever
R = radius of curvature
l = length of microcantilever
b = fixed end width of microcantilever
M = concentrated bending moment
I = area moment of inertia
κ = curvature
F_r = concentrated axial force
F_y = concentrated vertical force
dF_r = an increment of axial force
dF_y = an increment of vertical force
A = cross-sectional area
$Y(x,t)$ = deflection of microcantilever
$y(x)$ = vibration mode of microcantilever
t = time
ω = resonant angular frequency
U = maximum strain energy
T = maximum kinetic energy
f_{stress} = fundamental resonant frequency of curved triangular shaped mircocantilever as a function of surface stress
f_{str} = fundamental resonant frequency of straight triangular shaped microcantilever
f_{cur} = fundamental resonant frequency of curved triangular shaped microcantilever as a function of radius of curvature
f_{fem} = fundamental resonant frequency of curved triangular shaped microcantilever obtained by FEM analysis
f_{mod} = modified fundamental resonant frequency of curved triangular shaped microcantilever.
l/b = aspect ratio of triangular shaped microcantilever

1. Introduction

Microcantilevers have been widely used in chemical and biological detection[1-4] for their high sensitivity, fast response, reduced size and easy mass production at low cost.[5] Although they have been successful in biochemical detection, many researchers desire to

improve their performance by enhancing their mass sensitivity towards developing detection capabilities through geometry modification. The results showed that triangular shaped microcantilevers have mass sensitivity by an order of magnitude over the simple rectangular shaped microcantilevers of similar dimensions.[6] Moreover, triangular shaped microcantilevers can also avoid twisting caused by turbulence of the surrounding medium.[7]

Microcantilevers bend in response to differential surface stress.[8] Surface stress can be induced in various ways, such as absorbed molecules, temperature changes, or charge (or potential) changes.[5] In the size domain of micro electro mechanical systems (MEMS), surface stress can be overwhelming and often play an important role in microstructures due to the increasing surface to volume ratio as microstructures shrink to microns or nanometers.[9-10] To date, many theoretical models and experimental methods have been undertaken to study surface stress and the effect of surface stress on microcantilevers.[5,9-14] In this field, Stoney[15] accomplished the pioneering work who derived a widely accepted simple quantitative relation linking the surface stress σ and radius of curvature R of a bending microcantilever, named as Sotney's equation,

$$\sigma = \frac{E^* d^2}{6R}, \tag{1}$$

where, d is the microcantilever's thickness, $E^* = E/(1-\nu)$ is the biaxial modulus, E and ν are elastic modulus and Poisson's ratio of the microcanilever, respectively. It is especially noted that the unit of surface stress is N/m and $\sigma > 0$ is tensile, which has been adopted by many researchers.[5,10-11,13-14,16] However, the physical meaning of the surface stress requires careful attention. Some researchers define surface stress as force per unit length,[11,13-14] while others define it as force per unit width.[5,10,16] In this paper, the surface stress is defined as force per unit width.

Despite increased interest in microcantilevers, there is no quantitative study about the effect of surface stress induced curvature on dynamic response of microcantilevers, especially the promising triangular shaped microcantilevers. In this paper, the surface stress induced curvature and the effect of curvature upon the dynamic behavior of triangular shaped microcantilevers are investigated. A remarkably precise analytical formula for calculating the fundamental resonant frequency of curved triangular shaped microcantilever is deduced. This useful analytical formula, convenient for practical applications, is validated with FEM results and raises a new perspective that, surface stress can be calculated from the fundamental resonant frequency of curved microcantilever using readily measurable microcantilever properties, such as its geometry, elastic modulus and density.

2. Theory

2.1 Surface stress induced curvature[10,13]

The triangular shaped microcantilever is considered with a constant thickness. For the sake of clarity and simplicity, this paper assumes surface stress exists only on the microcantilever's upper surface and uniformly distributed over the entire surface, as show in Fig. 1(a). The x-axis is oriented in the neutral axis of the straight triangular shaped microcantilever and the y-axis is perpendicular to the x-axis. The length , thickness and fixed end width of the microcantilever are denoted as l, d and b, respectively.

As shown in previous works, the effect of surface stress can be modeled as a concentrated bending moment M at the microcantilever's free end, as shown in Fig. 1(b).[10,13] Thus, the transverse deflection of the triangular shaped microcantilever for this model obeys the following governing equation:

$$E^* I \frac{d^2 y}{dx^2} = M \tag{2}$$

and the boundary conditions are given as

$$y(0) = 0, \qquad \frac{dy}{dx}(0) = 0. \tag{3}$$

where, I is the area moment of inertia. For a triangular shaped microcantilever, I and M are defined by a rectangle with varying width as:

$$I = \frac{bd^3(1-x/l)}{12}, \qquad M = \frac{\sigma bd(1-x/l)}{2}. \tag{4}$$

Equation (2) is solved by using integration and boundary conditions as follows:

$$y = \frac{3\sigma x^2}{E^* d^2}. \tag{5}$$

For linear analysis of small deflection, the curvature κ of bending microcantilever is approximated as d^2y/dx^2. Therefore, the curvature κ and the radius of curvature R are given as:

$$\kappa = \frac{1}{R} = \frac{d^2 y}{dx^2} = \frac{M}{E^* I} = \frac{6\sigma}{E^* d^2}. \tag{6}$$

From equation (6), it is obvious that the modelling of the surface stress effect as a concentrated moment at the triangular shaped microcantilever's free end guarantees that the microcantilever has a constant curvature.

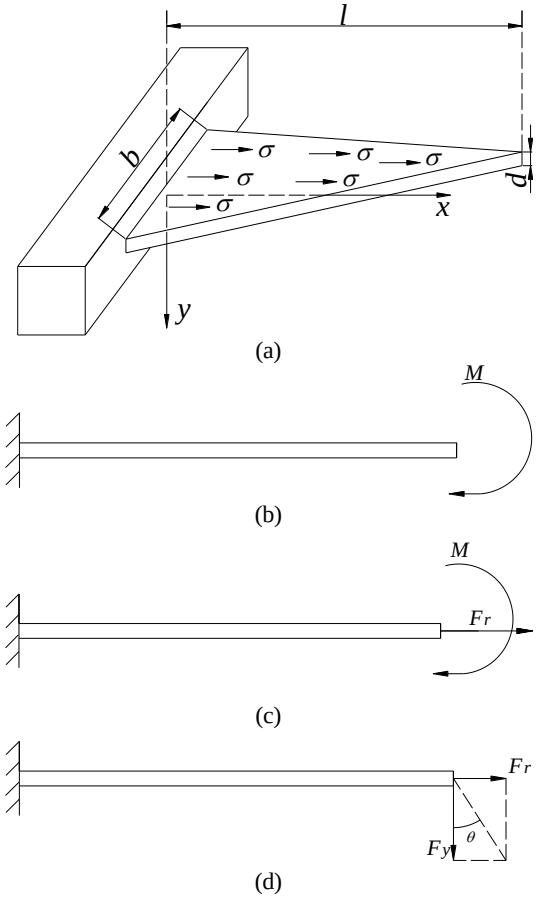

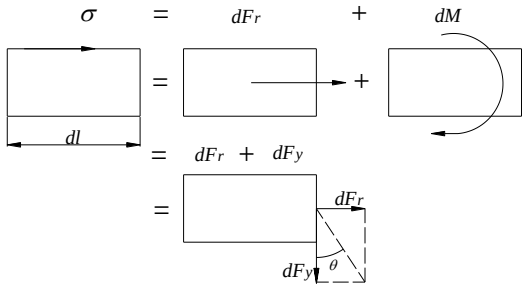

(e)

Fig. 1 Schematic of a theoretical model of triangular shaped microcantilever, (a) with surface stress, (b) with concentrated bending moment, (c) with concentrated bending moment and concentrated axial force, (d) with concentrated axial force and concentrated vertical force, (e) with decomposition.

The surface stress effect can be also modeled as a corresponding concentrated bending moment M plus a corresponding concentrated axial force F_r at the microcantilever's free end, as shown in Fig. 1(c). Further, this paper models the surface stress effect as a concentrated axial force F_r plus a concentrated vertical force F_y at the microcantilever's free end, as shown in Fig. 1(d). On any given microcantilever element sufficiently far from the fixed end the surface stress will impose an increment of an equivalent axial force dF_r and an increment of vertical force dF_y, this decomposition as shown in Fig. 1(e) (note that this is not a free-body diagram). The relationship between dF_r amd dF_y is given as:

$$dF_r = dF_y \times \tan\theta = \frac{\partial y}{\partial x} \times dF_y. \tag{7}$$

And the increment of vertical force dF_y is given as:

$$dF_y = \partial \frac{\sigma bd(1-x/l)}{2l}. \tag{8}$$

Substituting equation (8) into equation (7), the equivalent concentrated axial load per unit length is derived as:

$$\frac{dF_r}{dx} = \frac{\partial}{\partial x}\left[\frac{\sigma bd(1-x/l)}{2l} \times \frac{\partial y}{\partial x}\right]. \tag{9}$$

It is assumed that the vertical force will not affect the resonant frequency because it puts one half of the microcantilever into compression and the other half into tension in a symmetric manner, thus the effects will be ignored. In contrast to that, the axial load that represents the surface stress will tend to stretch or compress the microcantilever, which will increase or decrease its resonant frequency for any given bending mode.[13]

2.2 Dynamic response of curved triangular shaped microcanti levers[12,17]

Considering the axial load the governing equation for free transverse vibration of triangular shaped microcantilever can be written as:

$$EI\frac{\partial^4 Y}{\partial x^4} + \frac{\partial}{\partial x}\left[\frac{\sigma bd(1-x/l)}{2l} \times \frac{\partial Y}{\partial x}\right] + \rho A\frac{\partial^2 Y}{\partial t^2} = 0, \tag{10}$$

where, ρ is the density of the microcantilever, A is the cross-sectional area given by:

$$A = bd(1-x/l). \tag{11}$$

The deflection $Y(x,t)$ is assumed as $Y(x,t) = y(x)\exp(i\omega t)$, where $y(x)$ is the vibration mode and ω is the resonant angular frequency.

The boundary conditions for the microcantilever can be expressed as $y(0) = 0$, $y'(0) = 0$, $y''(l) = 0$, $y'''(l) = 0$. The variational method[17] is employed to solve the problem for it is very difficult to find the exact the solutions for equation (10). The resonance conditions are found by setting $\delta(U\text{-}T) = 0$, where the maximum strain energy U of a vibrating microcantilever is given as:

$$U = \frac{1}{2}\int_0^l EI\left(\frac{\partial^2 y}{\partial x^2}\right)^2 dx + \frac{1}{2}\int_0^l \frac{\sigma bd(1-x/l)}{2l}\left(\frac{\partial y}{\partial x}\right)^2 dx \tag{12}$$

and the maximum kinetic energy T of the microcantilever is given by:

$$T = \frac{\omega^2}{2}\int_0^l \rho A y^2(x)dx, \tag{13}$$

using $\partial^2 Y/\partial t^2 = -\omega^2 y(x)$. Here the vibration mode $y(x)$ can be expressed as a polynomial:

$$\begin{aligned} y(x) &= a_0 + a_1 x + c_1 x^2 + c_2 x^3 \\ &= c_1\psi_1 + c_2\psi_2. \end{aligned} \tag{14}$$

According to the boundary conditions, the $a_0 = a_1 = 0$, and we set $\psi_1 = x^2$ and $\psi_2 = x^3$. The two necessary conditions are $d(U/T)/dc_j = 0$, for $j = 1,2$. Let

$$r_{i,j} = \int_0^l \left(EI\frac{d^2\psi_i}{dx^2}\frac{d^2\psi_j}{dx^2} + \frac{\sigma bd(1-x/l)}{2l}\frac{d\psi_i}{dx}\frac{d\psi_i}{dx}\right)dx \tag{15}$$

and

$$s_{i,j} = \int_0^l \rho_s A\psi_i\psi_j dx \tag{16}$$

for $i, j = 1,2$. To have nontrivial solutions for c_k, the determinant must vanish, i.e.,

$$\left| r_{i,j} - \omega^2 s_{i,j} \right| = 0 \qquad \text{for } i, j, k = 1,2. \tag{17}$$

By solving equation (17), the fundamental resonant frequency of curved triangular shaped mircocantilever can be found as a function of the surface stress,

$$f_{stress} = \frac{\omega}{2\pi} = \frac{1}{2\pi l^2}\sqrt{\frac{1}{\rho}\left(\begin{array}{l}\frac{147}{10}\sigma l + \frac{119}{2}Ed^2 \\ -\frac{7}{10}\sqrt{\begin{array}{l}261\sigma^2 l^2 + \\ 2370\sigma lEd^2 + 6225E^2 d^4\end{array}}\end{array}\right)}. \tag{18}$$

Equation (18) raises a new perspective that, surface stress can be calculated from the fundamental resonant frequency of curved microcantilever using readily measurable microcantilever properties, such as its geometry, elastic modulus and density. This may be of great value for frequency-based surface stress measurements.

When $\sigma = 0$ equation (18) returns the expression for a free micircantilever (straight microcantilever), that is there is no surface stress on the microcantilever's surface. The fundamental resonant frequency of a straight triangular shaped microcantilever is given as:

$$f_{str} = \frac{d}{2\pi l^2}\sqrt{(\frac{119}{2} - \frac{7\sqrt{249}}{2})\frac{E}{\rho}} \approx 0.3289\frac{d}{l^2}\sqrt{\frac{E}{\rho}}. \tag{19}$$

Substituting equation (1) into equation (18), the fundamental resonant frequency of the curved triangular shaped microcantilevers is given as:

$$f_{cur} = \frac{d}{2\pi l^2}\sqrt{\frac{E}{\rho R(\nu-1)}\left(\begin{array}{l}\frac{119}{2}\nu R - \frac{49}{20}l - \frac{119}{2}R \\ -\frac{7}{20}\sqrt{\begin{array}{l}24900\nu^2R^2 - 1580l\nu R \\ -49800\nu R^2 + 29l^2 \\ +1580lR + 24900R^2\end{array}}\end{array}\right)}. \tag{20}$$

Although equation (19) and (20) hold quite well for a narrow microcantilever, they fail to take account for the Poisson's effect for a wider cantilever. If the fundamental resonant frequency of straight triangular shaped microcantilever f_{fem} is accurately known, then Poisson's effect can be weakened by the following modified equation

$$f_{mod} = \frac{f_{cur}}{f_{str}} f_{fem}, \quad (21)$$

where, f_{mod} is the modified fundamental resonant frequency of curved microcantilever.

3. Experimental procedure

To investigate the effect of surface stress induced curvature on the dynamic response of triangular shaped microcantilevers, modal analysis was performed using ANSYS software on the curved triangular shaped microcantilevers and straight triangular shaped microcantilevers. In these finite element analyses, the material properties were kept the same for all microcantilevers studied while varying the radius of curvature. The material properties include elastic modulus of 130 GPa, density of 2330 kg/m^3 and Poisson's ratio of 0.28. For usual microcantilevers, the microcantilever length often falls in a range of 100 to 500 μm, thickness varies from 0.5 to 2 μm[1,5,12,16,18-21] and aspect ratio $l/b > 1$. Following are the geometrical parameters used for the modeling of microcantilevers:

- Radius of curvature varied from 1 mm to 20 mm
- Lengths of the triangular shaped microcantilevers were 200, 500 μm
- Width of the triangular shaped microcantilevers was 100 μm
- Thickness of the triangular shaped cantilevers was 2 μm

It should be pointed out that the surface stress existing on the 200 μm long microcantilevers is tensile, while the 500 μm long microcantilevers is compressible.

4. Results and discussions

We now present numerical results and FEM results for the dynamic behavior of the triangular shaped microcantilevers. Fig. 2 presents results obtained by using equation (19) for the fundamental resonant frequency of the straight triangular shaped microcantilever and equation (20), (21) and FEM analysis for the fundamental resonant frequency of the curved triangular shaped microcantilevers with the material properties and dimensions except the radius of curvature.

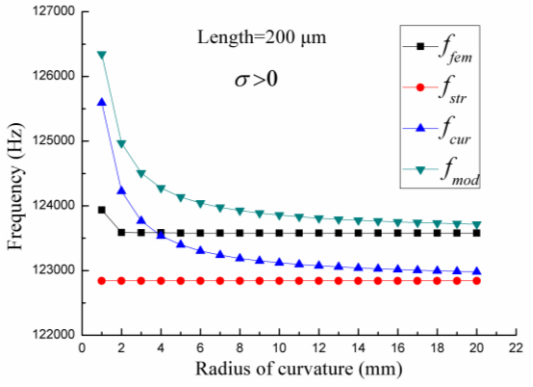

(a)

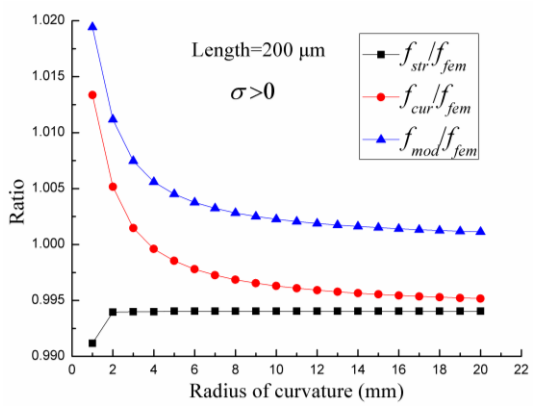

(b)

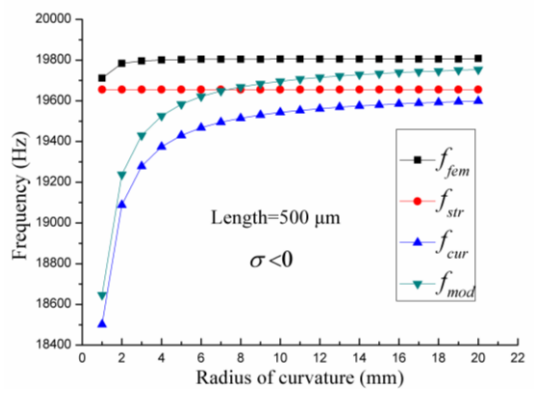

(c)

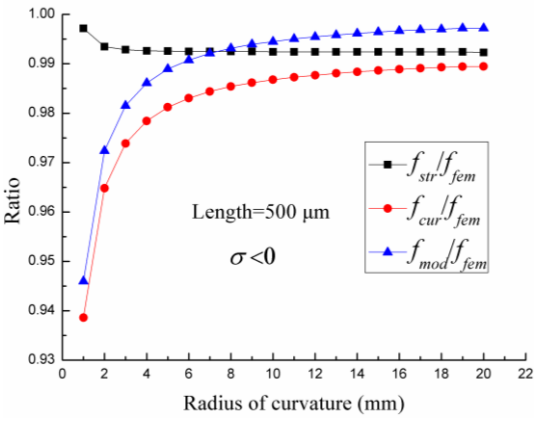

(d)

Fig. 2 Frequency and ratio results for the microcantilevers, the subscripts fem, str, cur and mod denote results obtained using FEM method, equation (19), equation (20) and equation (21), respectively. (a) the frequency results for the 200 μm long triangular shaped microcantilevers, (b) FEM results used as benchmark, the ratio results for the 200 μm long triangular shaped microcantilevers, (c) the frequency results for the 500 μm long triangular shaped microcantilevers, (d) FEM results used as benchmark, the ratio results for the 500 μm long triangular shaped microcantilevers.

The results presented in Fig. 2 can also be used to assess the accuracy of equation (19), (20) and (21). As shown in Fig. 2(a), the fundamental resonant frequency of the microcantilever given by FEM analysis, equation (20) and (21), decreases as the radius of curvature increases. In contrast to that, as the radius of curvature increases, the fundamental resonant frequency of the microcantilever obtained by FEM analysis, equation (20) and (21), increases as shown in Fig. 2(c). Note that for large radius of curvature (R > 20 mm), the results accorded by equation (21) are much closer to that of FEM analysis than those of the results of equation (19) and (20), as shown in Fig.

2(b) and Fig. 2(d). And the ratio of f_{mod} to f_{fem} is nearly 1. When R > 20 mm, the prediction of equation (19) are indistinguishable from that of equation (20). The reason may be that as the radius of curvature increases, the surface stress existing on the microcantilever's surface decreases. This can also get from equation (1). And then triangular shaped microcantilever begins to transform from curved-cantilever-like to straight-cantilever-like. For large radius of curvature, the surface stress is nearly zero. Thus the equation (20) returns to equation (19) that is the expression for a straight triangular shaped microcantilever. Clearly, the modified formula equation (21) is of great value to ignore the Poisson's effect, so the results can describe the dynamic behavior of the microcantilever much more accurately. Moreover, the assumption that the tensible force (σ > 0) or compressible force (σ > 0) will stretch or compress the microcantilever, which will increase or decrease its resonant frequency, is confirmed, as shown in Fig. 2(a) and Fig. 2(c).

As shown in Fig. 2(b), for the 200 μm long triangular shaped microcantilever, the maximum error of the results given by equation (19), (20) and (21) is 0.88%, 1.34% and 1.94%, respectively. When R > 20 mm the maximum error is not exceeding 0.6%, 0.48% and 0.11%, respectively. In contrast to that, for the 500 μm long microcantilever, the maximum error of the results of equation (19), (20) and (21) is 0.77%, 6.14% and 5.4%, respectively. When R > 20 mm the maximum error is within 0.77%, 1.06% and 0.28%, respectively, as shown in Fig. 2(d). The reason for the maximum error as high as 6.14% for large curvature can be attributed to deviation of the assumption that the deflection of the microcantilever bending is small and linearly proportional to the surface stress. For large curvature, the deflection becomes nonlinear and produces stiffening effect in the microcantilever. The stiffening effect in the microcantilever increases its bending stiffness, resulting in increased frequency in the microcantilever.

Consequently, we recommend the equation (20) when concerning effect of surface stress induced curvature on the dynamic response of the triangular shaped microcantilevers. Further, if the fundamental resonant frequency of the straight triangular shaped microcantilever with the same material properties and dimensions is accurately known, equation (21) should be used. Otherwise, if the effect of surface stress on change of resonant frequency of a microcantilever is not a concern, the fundamental resonant frequency of the curved triangular shaped microcantilever can be calculated by equation (19) for the sake of simplicity.

5. Conclusions

A detailed theoretical study of the effect of surface stress induced curvature on the dynamic response of triangular shaped microcantilever has been presented. This involved the derivation of analytical formulas for surface stress induced curvature and the fundamental resonant frequency of triangular shaped microcantilevers as a function of the curvature.

Surface stress is successfully modelled as a concentrated axial load plus a concentrated vertical force at the microcantilever's free end. The vertical force will not affect the resonant frequency of the microcantilever, whereas the axial load that represents the surface stress will tend to stretch or compress the microcantilever, which will increase or decrease its resonant frequency for any given bending mode.

The analytical formula for calculating the fundamental resonant frequency of curved triangular shaped microcantilevers agrees well with FEM results. It is therefore recommended that equation (20) should be used when concerning effect of surface stress induced curvature on the dynamic response of the triangular microcantilevers. Further, if the fundamental resonant frequency of the straight microcantilever with the same material properties and dimensions is accurately known, equation (21) should be used. This useful analytical formula, convenient for practical applications, raises a new perspective that surface stress can be calculated from the fundamental resonant frequency of curved microcantilever using readily measurable microcantilever properties, such as its geometry, elastic modulus and density.

ACKNOWLEDGEMENT

This research is supported by the Key Project of National Nature Science Foundation of China (No. 50836004 and No. 90923001) and the Fundamental Research Funds for the Central Universities (No. xjj20100140).

REFERENCES

1. Arntz, Y., Seelig, J. D., Lang, H. P., Zhang, J., Hunziker, P., Ramseyer, J. P., Meyer, E., Hegner, M. and Gerber, Ch., "Label-free Protein Assay Based on A Nanomechancial Cantilever Array," Nanotechnology, Vol. 14, No. 1, pp. 86-90, 2003.
2. Lee, Y., Lee, E. K., Cho, Y. W., Matsui, T., Kang, I. C., Kim, T. S. and Han, M. H., "ProteoChip: A Highly Sensitive Protein Microarray Prepared by A Novel Method of Protein, Immobilization for Application of Protein-protein Interaction Studies," Proteomics, Vol. 3, No. 12, pp. 2289-2304, 2003.
3. Berger, R., Delamarche, E., Lang, H. P., Gerber, C., Gimzewski, J. K., Meyer, E. and Guntherodt, H. J., "Surface Stress in the Self-assembly of Alkanethiols on Gold," Science, Vol. 276, No. 5321, pp. 2021-2024, 1997.
4. Lavrik, N. V., Sepaniak, M. J. and Datskos, P. G., "Cantilever Transducers as A Platform for Chemical and Biological Sensors," Review of Scientific Instruments, Vol. 75, No. 7, pp. 2229-2253, 2004.
5. Li, X. F. and Peng, X. L., "Theoretical Analysis of Surface Stress for A Microcantilever with Varying Widths," Journal of Physics D: Applied Physics, Vol. 41, No. 6, pp. 1-10, 2008.
6. Morshed, S. and Prorok, B. C., "Tailoring Beam Mechanics Towards Enhancing Detection of Hazardous Biological Species," Experimental Mechanics, Vol. 47, No. 3, pp. 405-415, 2007.
7. Miyatani, T. and Fujihira, M., "Calibration of Surface Stress Measurements with Atomic Force Microscopy," Journal of Applied Physics, Vol. 81, No. 11, pp. 7099-7115, 1997.
8. Jeon, S. and Thundat, T., "Instant curvature measurement for

microcantilever sensors," Applied Physics Letters, Vol. 85, No. 6, pp. 1083-1084, 2004.

9. Wang, G. F. and Feng, X. Q., "Effects of Surface Elasticity and Residual Surface Tension on the Natural Frequency of Microbeams," Applied Physics Letters, Vol. 90, No. 23, pp. 231904-1-3, 2007.
10. Zhang, Y., Ren, Q. and Zhao, Y. P., "Modelling Analysis of Surface Stress on A Rectangular Cantilever Beam," Journal of Physics D: Applied Physics, Vol. 37, No. 15, pp. 2140-2145, 2004.
11. Chen, G. Y., Thundat, T., Wachter, E. A. and Warmack, R. J., "Adsorption-induced Surface Stress and Its Effects on Resonance Frequency of Microcantilevers," Journal of Applied Physics, Vol. 77, No. 8, pp. 3618-3622, 1995.
12. Hwang, K. S., Eom, K., Lee, J. H., Chun, D. W., Cha, B. H., Yoon, D. S., Kim, T. S. and Park, J. H., "Dominant Surface Stress Driven by Biomolecular Interactions in the Dynamical Response of Nanomechanical Microcantilevers," Applied Physics Letters, Vol. 89, No. 17, pp. 173905-1-3, 2006.
13. McFarland, A. W., Poggi, M. A., Doyle, M. J., Bottomley, L. A. and Colton, J. S., "Influence of Surface Stress on the Resonance Behavior of Microcantilevers," Applied Physics Letters, Vol. 87, No. 5, pp. 053505-1-3, 2005.
14. Ren, Q. and Zhao, Y. P., "Influence of Surface Stress on Frequency of Microcantilever-based Biosensors," Microsystem Technologies-micro-and Nanosystems-information Storage and Processing Systems, Vol. 10, No. 4, pp. 307-314, 2004.
15. Stoney, G. G, "The Tension of Metallic Films Deposited by Dlectrolysis," Proceedings of the Royal Society of London Series A-containing Papers of A Mathematical and Physical Character, Vol. 82, No. 553, pp. 172-175, 1909.
16. Fernando, S., Austin, M. and Chaffey, J., "Improved Cantilever Profiles for Sensor Elements," Journal of Physics D: Applied Physics, Vol.40, No. 24, pp. 7652-7655, 2007.
17. Chen, G. Y., Warmack, R. J., Thundat, T. and Allison, D. P., "Resonance Response of Scanning Force Microscopy Cantilevers," Review of Scientific Instruments, Vol. 65, No. 8, pp. 2532-2537, 1994.
18. Ansari, M. Z., Cho, C., Kim, J. and Bang, B., "Comparison between Deflection and Vibration Characteristics of Rectangular and Trapezoidal profile Microcantilevers," Sensors, Vol. 9, No. 4, pp. 2706-2718, 2009.
19. Hansen, K. M. and Thundat, T., "Microcantilever Biosensors," Methods, Vol. 37, No. 1, pp. 57-64, 2005.
20. Raiteri, R., Grattarola, M., Butt, H. J. and Skládal P., "Micromechanical Cantilever-based Biosensors," Sensors and Actuators B, Vol. 79, No. 2-3, pp. 115-126, 2001.
21. Zhang, J., Lang, H. P., Huber, F., Bietsch, A., Grange, W., Certa, U., McKendry, R., Guntgerodt, H. J., Hegner, M. and Gerber, C., "Rapid and Label-free Nanomechanical Detection of Biomarker Transcripts in Human RNA," Nature Nanotechnology, Vol. 1, No. 3, pp. 214-220, 2006.